Published in AJSE, Vol:21, Issue: 1
Received on 24th August 2021
Revised on 27th December 2021
Accepted on 31th January 2022

AIUB JOURNAL OF SCIENCE AND ENGINEERING
**ISSN: 1608 – 3679 (print) 2520 – 4890 (Online)**

# Emergency Distribution Network Design & Analysis for Consecrated COVID 19 Hospital Zone

Abu Hena MD Shatil, *Member, IEEE*, and MD. Lutfur Rahman

***Abstract*— A power distribution network is always a key topic in a grid system because of more complexity. Rapidly or sudden load increasing to a particular one or two feeders can arise uncertainty and unbalance conditions in the system. Voltage fluctuations, Deviations, THD (total harmonic distortion), Reactive power imbalances can seriously unstable the grid for load increasing situations. In recent days due to COVID 19 condition, dedicated hospitals are connected to the distribution network. Because of its urgency and usefulness, a new type of distribution network called loop plus parallel has been presented in this paper. Finally, the simulation studies show better performance when comparing the traditional types of networks. New distribution network shows promising values in THD, Voltage deviation and also for reactive power imbalance.**

***Index Terms*—COVID 19, Power Distribution Networks, Loop plus parallel network, voltage fluctuation, THD, Deviations, Reactive power imbalance, Augmented Lagrange Multiplier**

## I. Introduction

COVID 19 is right now a burning topic. This microscopic virus deteriorates the whole national health care system. The disease's devastation has been seen in nearly every area and industry of the globe. According to WHO data, approximately 9.6 million individuals in 216 countries, regions, or territories were verified to be contaminated with the virus between June 28, 2020, and more than 491,000 lives were lost because of the sickness. Many nations have implemented different social distancing measures, and even as travel bans, city lockdowns, and work-from-home policies, to slow the spread of the disease [1].

The epidemic has a huge influence on the economy, society, and everyday life of individuals. Meanwhile, the power sector has been severely damaged and is facing significant challenges. Due to the restrictions, large power users, such as industries and commercial buildings, are compelled to shut down or operate at reduced capacity. As individuals are forced to remain at home, the residential load begins to take on a higher proportion. This shift in working and living styles has a substantial impact on the volume, profile, composition, and distribution of energy consumption. Changes in load distribution can influence the operation and control of the power system. Due to the pandemic's unusual development and rapidly altering anti-epidemic measures, the functioning of the power grid is likewise more unpredictable. Additionally, the lockout policy and disruption of the supply chain provide a direct impediment to asset maintenance and management [2],[3].

As like in many other countries, Bangladesh also took some steps to prevent the spread of the disease. One of the steps is to introduce new hospital only for COVID 19 patients. DNCC COVID 19 hospital in Mohakhali, Dhaka is the finest example of this pace. With 1,100 beds for serving coronavirus infected people, it is the largest Covid-19 hospital in Bangladesh right now. Of the 1,100 beds, 850 have oxygen support, while the other 250 beds have been installed as ICUs and HDUs. A total of 250 beds will be available at the initial stage, including 150 general beds with oxygen supply, 50 ICU beds and 50 emergency beds with high-flow nasal cannulas. As corona virus situation is fluctuating right now, so it's a prediction that this type of emergency dedicated hospital will increase to near future [4].

These large, complicated emergency hospitals required a new shape of distribution network. As stated earlier, these hospitals will use very sophisticated biomedical instrumentation and power tools, so power flow condition, reactive power balance, voltage fluctuations will be the crucial area to design. Nowadays Parallel Main units are widely used in Metro cities and smart cities for providing reliable supply to the consumers. A Parallel Main Network is formed by connecting feeders in a fashion to form a loop and is fed at one or several points. The main aim of this parallel main network is to provide consumer's uninterrupted supply. This is possible by feeding consumers with another healthy feeder in case of loss of supply due to working feeder. If a fault occurs in any branch of sub transmission circuit, that branch is removed from service and power continues from the remaining loop without discontinuity in the supply. Every consumer has redundant supply in Ring main distribution system. Parallel is very

Abu Hena MD Shatil is with the Department of Electrical & Electronic Engineering, American International University Bangladesh. (email: abu.shatil@aiub.edu)
MD. Lutfur Rahman is with the Bangladesh Technical Education Board (BTEB). (email: md.lutfurrahmanabrar@gmail.com)

expensive and requires more materials than other distribution system. High maintenance cost and it is not usable when the client is located at the center of the load.

This paper analyzes a new power distribution network loop plus parallel, especially for emergency hospital zone, with the help of the Augmented Lagrange Multiplier algorithm. Comparing with parallel network feeder, loop plus parallel feeder shows promising result.

## II. Distribution Network Design

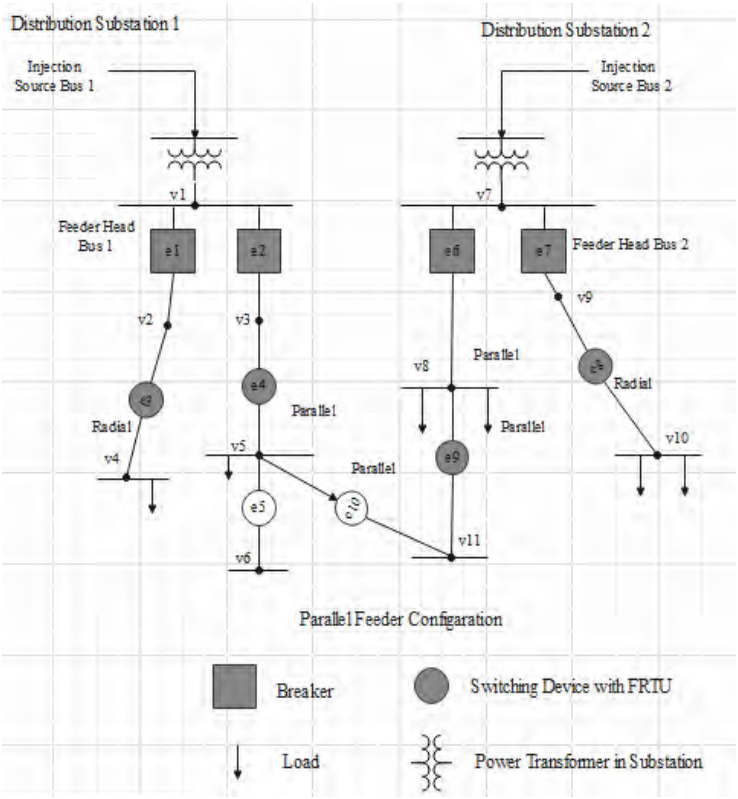


Fig. 1. An interconnection between two feeders supplied by two distinct substations.

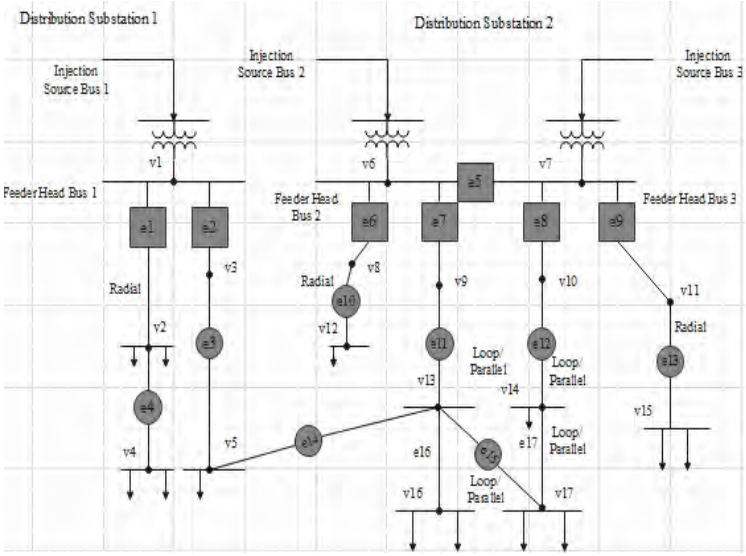


Fig. 2. combination of parallel plus loop feeder.

General distribution network is constructed by using parallel feeder combination. The Fig. 1. depicts an interconnection between two feeders supplied by two distinct substations. Parallel feeder configurations are frequently utilized in large distribution network areas when huge loads must be serviced with a high degree of dependability. This setup establishes many utility services in simultaneously, resulting in a more dependable system [5]. The advantage of this arrangement is that it allows for the failure of a single transformer without causing additional service interruptions in that section of the system. The system's electricity can be provided via the secondary injection source via the distribution substation's tie switch.

Fig. 2. Illustrates new type of distribution network which is a combination of parallel plus loop feeder. The three injection source buses with three transformers facilitate the power injection in this arrangement. Additionally, because the system may rely on two distinct substations, this interim arrangement is built in such a way that its performance must adhere to system circumstances and restrictions. In this network interconnected feeders with ties switches and NO switches will be operated from the optimum network condition. When feeders are energized from different substation then parallel configuration will take place along with the loop feeder configuration.

## III. Mathematical Modelling

In this research paper Augmented Lagrange Multiplier method has been used.

### A. Equations

ALM method may be called as Method of Multiplier (MOM) or Primal-Dual Method. Let's consider Lagrangian functional only for equality constraints.

$$L(x) = f(x) + \lambda^T h(x) \quad (1)$$

In order to avoid the unboundness of Lagrangian, a penalty function is introduced. We call it as augmented Lagrangian $A(x, \lambda, \mathrm{r}) = L(x, \lambda) + \frac{1}{2}\sum_{i=1}^{i} r_i h_i(x)^2$ where, $r_i$ is the penalty parameter for the ith equality constraint. In the ALM method, the unconstrained optimization tool sequentially minimizes the augmented Lagrangian for the given value of $r_i$ and $\lambda_i$. Then, these two parameters are modified to satisfy the optimality condition. The update rule for Lagrange multipliers can be determined from the following relation [6].

$\lim_{x \to x} A(x, \lambda, r) = \nabla L(x^*, \lambda^*)$

This implies

$$\lim_{x \to x} (\lambda_i + r_i h_i(x)) = \lambda_i^*, i = 1,2, \dots, l. \quad (2)$$

Hence, the update rule for Laqrange multipliers is

$\lambda_i^{k+1} = \lambda_i^k + r_i^k h_i(x^k), i = 1,2, \dots, l$

where, the superscript $k$ is the iteration of ALM algorithm.

Inequality constraints are transformed into equality constraints by adding slack variables$(\theta_j > 0)$. Thus, the augmented Lagrangian becomes

$$A(\mathbf{x}, \boldsymbol{\theta}, \boldsymbol{\mu}, \mathbf{r}) = f(\mathbf{x}) + \sum_{j=1}^{m} \left[\mu_j\big(g_j(\mathbf{x}) + \theta_j\big) + \frac{1}{2} r_j \big(g_j(\mathbf{x}) + \theta_j\big)^2\right]$$

Then, new primal variables are $\bar{x} = \{x, \theta\}$ The augmented Lagrangian should satisfy the optimality condition for slack variable $\theta_j$

$$\nabla_{\theta 1} A(\mathbf{x}, \theta, \mu, \mathbf{r}) = \sum_{j=1}^{m} \left(\mu_j + r_j\big(g_j(\mathbf{x}) + \theta_j\big)\right) = 0 \qquad (3)$$

Hence, an optimum of slack variable $\theta_j$ is

$$\theta_j^* = \max\left\{0, -\frac{\mu_j}{r_j} - g_j(\mathbf{x})\right\}.$$

Now, these optimum values are substituted into the originally transformed form.

$$g_j(x) + \theta_j^* = g_j(\mathrm{x}) + \max\left\{0, -\frac{\mu_j}{r_j} - g_j(\mathbf{x})\right\} = \max\left\{g_j(x), -\frac{\mu_j}{r_j}\right\}$$

Hence, the augmented Lagrangian for inequality constraints are transformed into the following simple functional.

$$A(\mathbf{x}, \boldsymbol{\mu}, \mathbf{r}) = f(\mathbf{x}) + \sum_{-1}^{m} \left[\mu_j \Psi_j\big(\mathbf{x}, \mu_j, r_j\big) + \frac{1}{2} r_j \Psi_j\big(\mathbf{x}, \mu_j, r_j\big)^2\right] \qquad (4)$$

$$\Psi_j\big(\mathbf{x}, \mu_j, r_j\big) = \max\left\{g_j(\mathbf{x}), -\frac{\mu_j}{r_j}\right\} \qquad (5)$$

Also, the Lagrange multiplier update rule is defined as

Where,

$$\mu_j^{k+1} = \mu_j^k + r_j \Psi_j\big(\mathbf{x}^k, \mu_j^k, r_j^k\big), j = 1,2, \dots, l$$

C1. The gradients $\nabla f_i(x^*), i = 1, \dots, r$ and $\nabla g_j(x^*), j = 1, \dots, q$ are linearly independent; hence, there exists a unique Lagrange multiplier vector $w^* = (u^*, v^*) \in \mathbf{R}_+^p \times \mathbf{R}^q$ such that:

$$\nabla_x L(x^*, u^*, v^*) = \nabla f_0(x^*) - \sum_{i=1}^{P} u_i^* \nabla f_i(x^*) - \sum_{j=1}^{q} v_j^* \nabla g_j(x^*) = 0$$

C2. The Hessian of the Lagrangian $L(x, u, v)$ with respect to $x$ at$(x^*, u^*, v^*)$,

$$\nabla_{xx}^2 L(x^*, u^*, v^\star) = \nabla^2 f_0(x^*) - \sum_{i=1}^{P} u_i^* \nabla^2 f_i(x^*) - \sum_{j=1}^{q} v_j^* \nabla^2 g_j(x^*)$$

is positive definite on the affine subspace tangent to the feasible set at $x^*$; i.e.,

$$y^T \nabla_{xx}^2 L(x^*, u^*, v^*) y > 0,$$

For all $y \in Y \subset \mathbf{R}^n$, where

$$Y = \{y:\ y^T \nabla f_i(x^*) = 0, i = 1, \dots, r, y^T \nabla g_j(x^*) = 0, j = 1, \dots, q\} \qquad (6)$$

$$F(x, u, v, k) = \begin{cases} f_0(x) & -k^{-1}\sum_{i=1}^{p} u_i \ln\left(k f_i(x) + 1\right) \\ & -\sum_{j=1}^{q} v_j g_j(x) + k/2 \sum_{j=1}^{q} g_j^2(x), \quad \text{if } x \in \text{ int } \Omega_k \\ \infty, & \text{if } x \notin \text{ int } \Omega_k \end{cases}$$

Let us also define

$$h\big(x, t_{(p-r)}^u, k\big) = \sum_{t=r+1}^{P} \hat{u}_i(x, t_i^u, k) \nabla f_i(x) = k \sum_{i=r+1}^{p} t_i^u (k f_i(x) + 1)^{-1} \nabla f_i(x) \qquad (7)$$

It is clear that the vector-function $h\big(x, t_{(p-r)}^w, k\big)$ is smooth up to second-order and

$$h(x^*, 0, k) = 0, \quad \nabla_x h(x^*, 0, k) = 0^{n \times n}$$
$$\nabla_{i_0} h(x^*, 0, k) = 0^{n \times r}, \quad \nabla_i h(x^*, 0, k) = 0^{n \times q}$$

For $k > 0$, consider the mapping $\Phi_k\big(x, \hat{u}_{(r)}, \hat{v}, t\big)$: $\mathbf{R}^{n+r+p+2q} \to \mathbf{R}^{n+r+q}$ :

$$\Phi_k\big(x, \hat{u}_{(r)}, \hat{v}, t\big) = \begin{bmatrix} \nabla f_0(x) - \nabla f_{(r)}(x)^T \hat{u}_{(r)} - \nabla g(x)^T \hat{v} - h\big(x, t_{(p-r)}^u, k\big) \\ k^{-1}\big(k t_{(r)}^u + u_{(r)}^*\big)\big(k f_{(r)}(x) + e_r\big)^{-1} - k^{-1}\hat{u}_{(r)} \\ k^{-1}(k t^v + v^*) - g(x) - k^{-1}\hat{v} \end{bmatrix}$$

From condition Cl and the formulas for the Lagrange multiplier updates,

$$\Phi_k\big(x^*, u_{(r)}^*, v^*, 0\big) = 0$$

The Jacobian of $\Phi_k\big(x, \hat{u}_{(r)}, \hat{v}, t\big)$ with respect to $\big(x, \hat{u}_{(r)}, \hat{v}\big)$, at $\big(x, \hat{u}_{(r)}, \hat{v}, t\big) = \big(x^*, u_{(r)}^*,$
$v^*, 0\big)$

$$\nabla\Phi_k \equiv \nabla_{(x,\hat{u}_{(r)},\hat{t})}\left(\Phi_k\left(x^*,u^*_{(r)},v^*,0\right)\right)$$
$$= \begin{bmatrix} \nabla^2_{xx}L(x^*,u^*,v^*) & -\nabla_x f^T_{(r)}(x^*) & -\nabla_x g^T(x^*) \\ -U^*_{(r)}\nabla_x f_{(r)}(x^*) & -k^{-1}I^r & 0^{r\times q} \\ -\nabla_x g(x^*) & 0^{q\times r} & -k^{-1}I^q \end{bmatrix}$$

where $U^*_{(r)} = \text{diag}\,(u^*_i)^r_{i=1}$

$$\hat{u}_{(p-r)}(\cdot) \le \frac{u_{(p-r)} - u^*_{(p-r)}}{k\alpha/2}$$

or, since $u^*_{(p-r)} = 0$,

$$\left\|\hat{u}_{(p-r)}(\cdot) - u^*_{(p-r)}\right\| = \left\|\hat{u}_{(p-r)}(\cdot)\right\| \le 2\alpha^{-1}k^{-1}\left\|u_{(p-r)} - u^*_{(p-r)}\right\|.$$

From the implicit function theorem we have at $t = 0$

$$\nabla_t\left(x(t),\hat{u}_{(r)}(t),\hat{v}(t)\right)\Big|_{t=0} = -\nabla\Phi_k^{-1}\nabla_t\Phi_k\left(x^*,u^*_{(r)},v^*,t\right)\Big|_{t=0}. \quad (8)$$

Hence, for $t$ close enough to 0 it follows from the bound on $\nabla\Phi_k$,

$$\left\|\left(x(t),\hat{u}_{(r)}(t),\hat{v}(t)\right) - (x^*,u^*,v^*)\right\| \le 1 / \rho\left\|\Phi_k\left(x^*,u^*_{(r)},v^*,t\right) - \Phi_k\left(x^*,u^*_{(r)},v^*,0\right)\right\|$$

## IV. Result Analysis

Simulation for both the networks has done in MATLAB environment. Fig. 3. and 4 depicts the real power flow in bus 1 and in bus 2 for both loop and loop plus parallel condition. It has been seen from the picture that, for both of the cases loop plus parallel condition deliver more real power to the system because having 3 injection sources.

TABLE I
List of Parameters for Distribution Network

| Section Number | Node | Resistance (p.u) | Reactance (p.u) | Current Distribution Factor |
|---|---|---|---|---|
| 1 | 1-2 | 0.0058 | 0.0029 | 0.5 |
| 2 | 2-3 | 0.0308 | 0.0157 | 1.0 |
| 3 | 3-4 | 0.0228 | 0.0116 | 0.5 |
| 4 | 5-9 | 0.0238 | 0.0121 | 1.0 |
| 5 | 10-11 | 0.0511 | 0.0441 | 0.5 |
| 6 | 12-14 | 0.0117 | 0.0386 | 1.0 |
| 7 | 15-17 | 0.0118 | 0.0399 | 1.0 |

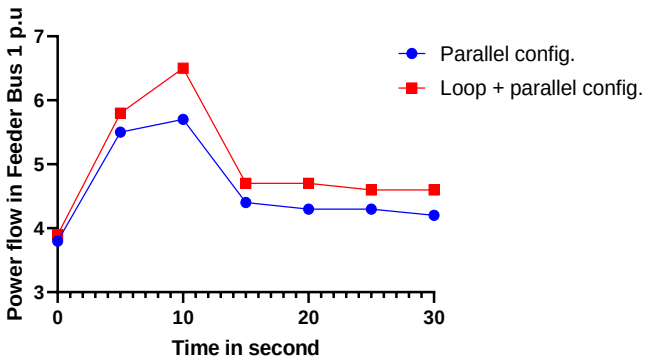


Fig. 3. Real power flow in bus 1

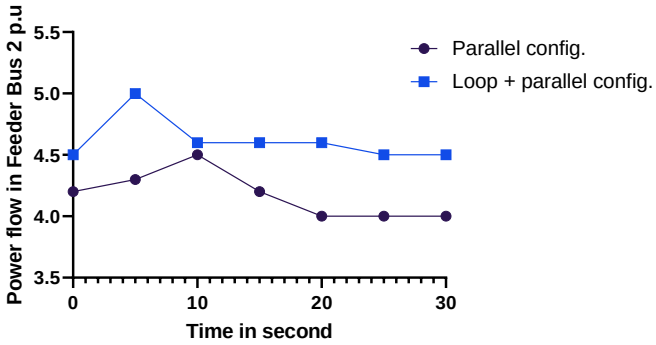


Fig. 4. Real power flow in Bus 2

Fig. 5 and 6 describes reactive power flow in bus 1 and 2. Its clearly seen that for both cases loop plus parallel network shows less fluctuation in reactive power. Also, it states less reactive power amplitude for loop plus parallel network.

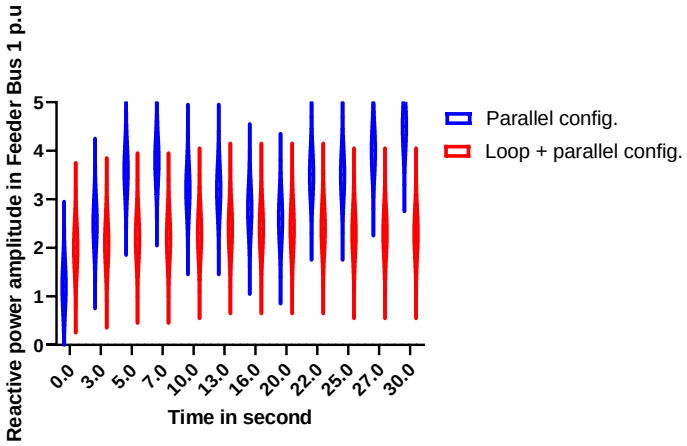


Fig. 5. Reactive power flow in bus 1

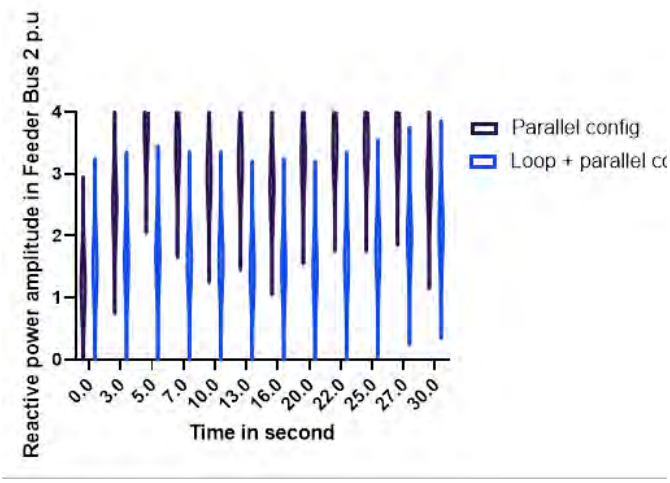


Fig. 6. Reactive power flow in bus 2

Fig. 7. discuss about total harmonic distortion (THD). Because of its switching device placement, loop plus parallel feeder configuration shows less harmonic distortion in percentage across time.

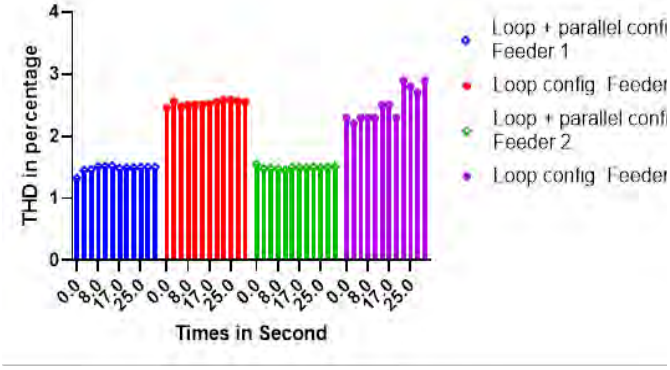


Fig. 7. THD values in different bus

Voltage fluctuation plays an important parameter to determining the bus quality. It's also related with THD as well. Less THD percentage will show less voltage fluctuations along the feeder. Fig. 8. shows a graph regarding the voltage fluctuation which has taken from the simulation. In that graph it is clearly observed that loop plus parallel network maintains a voltage fluctuation around 1.6% average which is acceptable for most of the distribution line standard. On the other hand, loop configuration shows higher fluctuation values which indicates instability in distribution network.

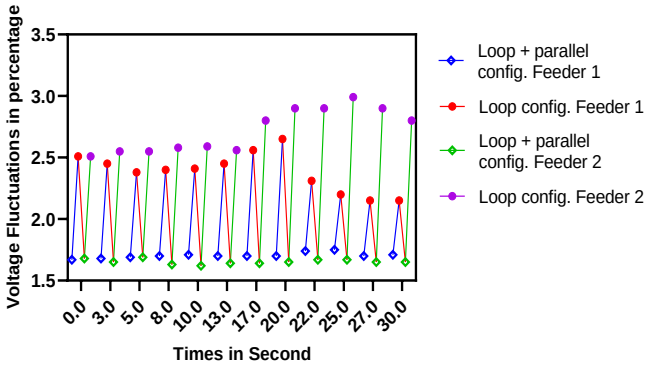


Fig. 8. Voltage fluctuations value in bus

Fig. 9. is about surge impedance loading data (SLD) versus voltage deviations. Surge impedance loading determines the loading ability of a distribution or transmission network. If the load value goes more than SLD values then voltage at the receiving start to get decrease. Loop plus parallel configuration shows less voltage deviation at the consumer when the SLD values increase by few percentages. But the loop configuration shows a high voltage deviation which is very harmful for most of the complex components connected with the distribution network. This mainly happens due to number of injection bus. Generally, less injection bus tends to find more imbalance in reactive power when the SLD increases, which leads more voltage deviation. This is what happens for parallel feeder configuration.

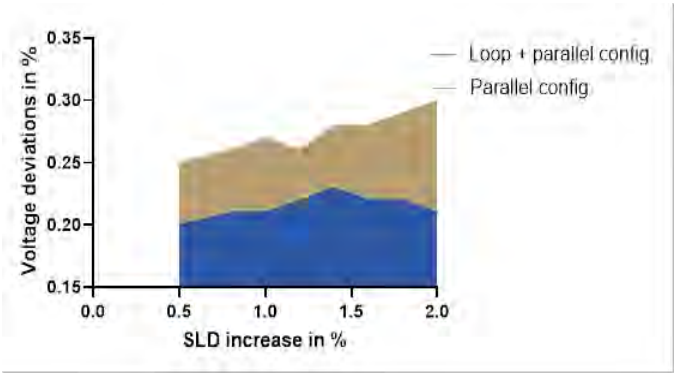


Fig. 9. Voltage deviation due to load increase

## V. SWITCHING PROCEDURE

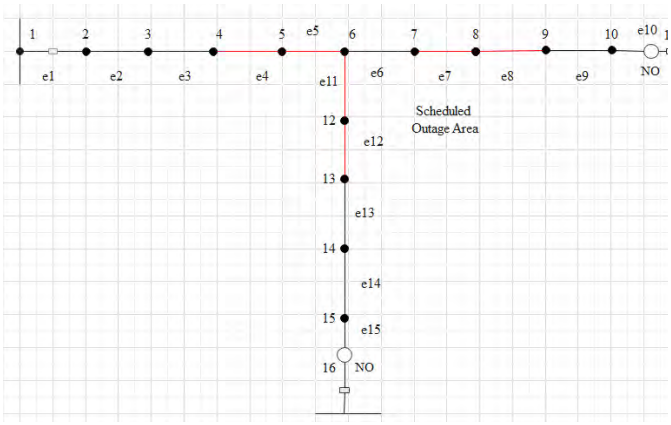


Fig. 10. complex network switching procedure

Fig. 10. illustrates a three-feeder arrangement for less complex network. Two usually open tie switches, e10 and e16, are linked to other feeds or substations. Disconnectors are represented by the e4, e5, e7, e8, e11, and e12 (non-remote-controlled switches). In this instance, the planned outage section is e6. The circuit breaker e1 is tripped in Step 1 (e10 and e15 remain open) to isolate the whole region initially. The team will next open e5, e7, and e11 to reduce the size of the outage region to the lowest possible. Step 3 reopens breaker e1 and tie switches e10 and e15 to restore service to unplanned areas.

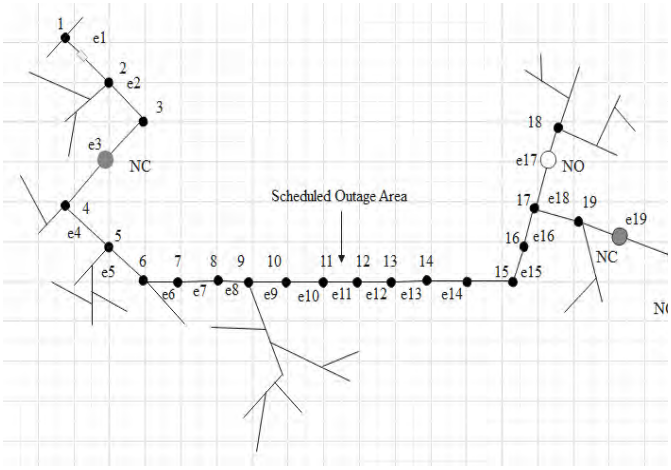


Fig. 11. Complicated network switching procedure

As shown in Fig. 11. a more complicated but more realistic example is presented. e11 is the planned outage section. Two visible tree topologies may be shown by dividing this topology in half along the planned outage section. e13 and e19 are Normally closed switch and will be operated remotely. The usually open tie switches (e17 and e20) are used to link the feeders or substations to one another. To prevent harming more customers, in Step 1, the boundary remote-controlled switches e3 and e19 are opened rather than triggering the breaker. Then e10 and e12 will be open to minimize the damage. In Step 3, the condition presupposes that shutting the tie switch e20 is the more economical and optimal choice for connecting neighboring feeders or substations (also, the operator can close e17 and e19 to restore the service).

## VI. CONCLUSION

In this paper, the loop plus parallel network feeder has been analyzed. Throughout the simulation, it has been seen that loop plus parallel network shows better power flow to the load. In the case of reactive power, the difference is minimal, but in the case of THD & voltage fluctuations, the parallel plus loop network delivers better results than the loop network. SLD simulation output is also crucial for network determination because it will actually show the performance of that particular network during the load increasing. In this situation, loop plus parallel feeder shows more minor deviation of voltage when a load is fluctuating, which certainly increase the credibility of the loop plus parallel network. Finally, a switching scheme has been shown in Fig. 10. and 11 which discuss about the routing of power during the major outage time.

## REFERENCES


[1] A. Navon, R. Machlev, D. Carmon, A. E. Onile, J. Belikov, and Y. Levron, "Effects of the COVID-19 Pandemic on Energy Systems and Electric Power Grids—A Review of the Challenges Ahead," *Energies*, vol. 14, no. 4, p. 1056, Feb. 2021.

[2] H. Zhong, Z. Tan, Y. He, L. Xie and C. Kang, "Implications of COVID-19 for the electricity industry: A comprehensive review," in *CSEE Journal of Power and Energy Systems*, vol. 6, no. 3, pp. 489-495, Sept. 2020

[3] D. Kai, L. Wei, H. Yuchuan, H. Yuchuan, H. Pan and Q. Yimin, "Power Quality Comprehensive Evaluation for Low-Voltage DC Power Distribution System," *2019 IEEE 3rd Information Technology, Networking, Electronic and Automation Control Conference (ITNEC)*, 2019, pp. 1072-1077

[4] "Bangladesh's largest Covid-19 hospital opens," *Dhakatribune.com*, 18-Apr-2021. [Online]. Available: https://www.dhakatribune.com/health/coronavirus/2021/04/18/health-minister-inaugurates-dncc-covid-19-dedicated-hospital. [Accessed: 24-Aug-2021].

[5] C.-W. Ten and Y. Tang, *Electric Power: Distribution Emergency Operation*. Boca Raton : Taylor & Francis, a CRC title, part of the Taylor &: CRC Press, 2018.

[6] "ALM," Functionbay.com. [Online]. Available: https://functionbay.com. [Accessed: 24-Aug-2021]



**Abu Hena MD Shatil** is an Assistant Professor of Electrical and Electronic Engineering (EEE) at American International University Bangladesh (AIUB). His work focuses specifically on the Energy modelling and their impact on society. He obtained Postgraduate degree in Electrical Energy System from Cardiff University, UK.



**Md Lutfur Rahman** finished BSc and MSc from AIUB in the field of Electrical and Electronic Engineering. His interest is in power system and Renewable energy. He iworking with Bangladesh Technical Education Board now.